Structures of $[Mg•(H_2O)_{1,2}]^+$ and $[Al•(H_2O)_{1,2}]^+$ ions studied by infrared photodissociation spectroscopy. Evidence of $[HO–Al–H]^+$ ion core structure in $[Al•(H_2O)_2]^+$

Yoshiya Inokuchi [a,*], Keijiro Ohshimo [a,1], Fuminori Misaizu [b], Nobuyuki Nishi [a]

[a]*Institute for Molecular Science, Myodaiji, Okazaki 444-8585, Japan*

[b]*Department of Chemistry, Tohoku University, Aoba-ku, Sendai 980-8578, Japan*

Abstract

Infrared spectra of $[Mg•(H_2O)_{1,2}]^+$ and $[Al•(H_2O)_{1,2}]^+$ are measured in the OH stretching region (3200–3800 cm^{-1}). The spectra show the symmetric and asymmetric OH stretching bands of water molecules that are directly bound to the metal ions through metal–oxygen intermolecular bonds. In addition to these bands, the $[Al•(H_2O)_2]^+$ ion has another band at 3714 cm^{-1}. This band is assigned to the free OH stretching vibration of the $[HO–Al–H]^+$ ion; the aluminum ion is inserted into the O–H bond of one water molecule in $[Al•(H_2O)_2]^+$.

[*]Corresponding Author. Fax: +81-564-55-7352. *E-mail address:* ino@ims.ac.jp (Y. Inokuchi).

[1]Present address: Chemical Dynamics Laboratory, RIKEN, Wako, Saitama 351-0198, Japan.

1. Introduction

Metal–water cluster ions in the gas phase are interesting models for fundamental interactions involved in metal–water bonding and metal ion solvation. For magnesium–water cluster ions, a number of experimental [1–5] and theoretical [6–11] studies have been devoted to investigating the structures and chemical reactions. Photodissociation spectra of the $[Mg•(H_2O)_1]^+$ ion in the 26000–40000 cm^{-1} region show bands due to the ^2P–^2S type transition of Mg^+ [1–4]. Duncan and co-workers demonstrated experimentally that the $[Mg•(H_2O)_1]^+$ ion has a geometric structure with C_{2v} symmetry, and that the symmetric and asymmetric OH stretching vibrations of the water molecule have frequencies of 3360 and 3632 cm^{-1}, respectively, in the excited $^2B_2$ state [2]. Fuke and co-workers extended the measurement of the electronic spectra of $[Mg•(H_2O)_n]^+$ to n = 5 [3,4]. According to the tendency of the band shift, they concluded that the first solvation shell closes at n = 3 [4]. Theoretically, ab initio molecular orbital (MO) calculations were done to obtain stable structures, binding energies, and harmonic frequencies of the Mg^+–water clusters [6–11]. As regards aluminum–water cluster ions, Misaizu et al. reported the photodissociation spectroscopy of $[Al•(H_2O)_{1–10}]^+$ in the 193–308 nm region [12]. They implied that the $[Al•(H_2O)_3]^+$ ion was stable in comparison with the $[Al•(H_2O)_{4,5}]^+$ ions on the basis of photofragmentation patterns. Theoretical investigations of $[Al•(H_2O)_n]^+$ were also done by several groups [7–17]. One of the noticeable results is that the $[HO–Al–H]^+$ ion core can be stable in the $[Al•(H_2O)_n]^+$ cluster ions [15,16].

As demonstrated in the previous reports [1–4,12], the electronic spectra provide quite valuable information on the electronic structures and the ion cores of the cluster ions. However, it is slightly difficult to obtain detailed aspects of geometric structures from these spectra. Vibrational spectroscopy is thought to be one of the

most powerful methods to determine structures. In particular, the infrared photodissociation spectroscopy is quite useful for cluster ions [18–22]. By measuring infrared photodissociation spectra, one can obtain vibrational frequencies and discuss cluster structures. Recently, Duncan and co-workers have been successfully demonstrating the solvation features of CO_2 or H_2O to metal ions with the infrared photodissociation spectroscopy and ab initio MO calculations [23–27].

In this letter, we report infrared spectra and structures of $[Mg•(H_2O)_{1,2}]^+$ and $[Al•(H_2O)_{1,2}]^+$ ions. Infrared photodissociation spectra of $[Mg•(H_2O)_{1,2}•Ar]^+$ and $[Al•(H_2O)_{1,2}•Ar]^+$ are measured by use of an ion guide spectrometer and a pulsed infrared laser. Duncan et al. suggested that the argon attachment to solvated metal ions hardly affects infrared spectra concerning band positions [25,26]. Therefore, it can be reasonably understood that the infrared photodissociation spectra of $[Mg•(H_2O)_{1,2}•Ar]^+$ and $[Al•(H_2O)_{1,2}•Ar]^+$ are equivalent to infrared spectra of $[Mg•(H_2O)_{1,2}]^+$ and $[Al•(H_2O)_{1,2}]^+$. Geometries of the $[Mg•(H_2O)_{1,2}]^+$ and $[Al•(H_2O)_{1,2}]^+$ ions are optimized and vibrational frequencies are evaluated by density functional theory (DFT) calculations.

2. Experimental and computational section

The infrared photodissociation spectra of $[Mg•(H_2O)_{1,2}•Ar]^+$ and $[Al•(H_2O)_{1,2}•Ar]^+$ are measured by use of an ion guide spectrometer with two quadrupole mass filters. Figure 1 shows a schematic diagram of the apparatus. The cluster ions are produced in the pick-up-type cluster source. Gas mixture of water (~ 1% content) and argon is introduced into the vacuum chamber through a pulsed nozzle (General Valve Series 9) with a 0.80 mm orifice diameter, a pulse duration of ~300 μs,

and a repetition rate of 10 Hz. The total stagnation pressure is 3×10^5 Pa. Metal ions are produced by laser irradiation of a rotating Mg or Al rod (6 mm diameter) that is located at 5 mm from the exit of the pulsed nozzle. The second harmonic (532 nm, 5 mJ/pulse) of a Nd:YAG laser (Spectra Physics INDI-50) is focused by a lens with a focal length of 300 mm. Neutral clusters pick up metal ions and produce solvated metal ions. After passing through a skimmer, cluster ions are introduced into the spectrometer with a 50 eV kinetic energy. Parent ions are isolated by the first quadrupole mass filter. After deflection by 90° through an ion bender, parent ions are led into a quadrupole ion guide. The ion beam is merged with a laser beam in the ion guide, and parent ions are excited into vibrationally excited states. The excitation induces fragmentation of parent ions. Resultant fragment ions are mass-analyzed by the second quadrupole mass filter, and detected by a secondary electron multiplier tube. For normalization of fragment-ion yields, the power of the dissociation laser is monitored by a pyroelectric detector (Molectron P1-15H-CC). Both ion signals from the ion detector and laser signals from the pyroelectric detector are fed into a digital storage oscilloscope (LeCroy 9314A) and averaged out. The oscilloscope is controlled by a microcomputer through the general purpose interface bus (GPIB). Infrared photodissociation spectra of parent ions are obtained by plotting normalized yields of fragment ions against wavenumber of the dissociation laser. Fragment ions monitored for the spectra of $[Mg\bullet(H_2O)_n\bullet Ar]^+$ and $[Al\bullet(H_2O)_n\bullet Ar]^+$ are $[Mg\bullet(H_2O)_n]^+$ and $[Al\bullet(H_2O)_n]^+$, respectively.

The tunable infrared source used in this study is an optical parametric oscillator (OPO) system (Continuum Mirage 3000) pumped with an injection-seeded Nd:YAG laser (Continuum Powerlite 9010). The output energy is 1–2 mJ/pulse, and the linewidth is approximately 1 cm^{-1}. The infrared laser is loosely focused by a CaF_2 lens

(a focal length of 1000 mm) located just before the spectrometer. The wavenumber of the OPO laser is calibrated by a commercial wavemeter (Burleigh WA-4500).

Moreover, the $[Mg•(H_2O)_{1,2}]^+$ and $[Al•(H_2O)_{1,2}]^+$ ions are analyzed by DFT calculations. The calculations are made with the Gaussian 98 program package [28]. Geometry optimization and vibrational frequency evaluation are carried out at the B3LYP/6-31+G* level of theory. For calculated vibrational frequencies, we use a scaling factor of 0.9654 for comparison of calculated infrared spectra with observed ones.

3. Results and discussion

Figure 2 shows a schematic drawing of optimized structures of $[Mg•(H_2O)_{1,2}]^+$ and $[Al•(H_2O)_{1,2}]^+$. For both $[Mg•(H_2O)_1]^+$ and $[Al•(H_2O)_1]^+$, Form 1-I (Fig. 2a) is stable. It has the C_{2v} symmetry, and distances between the metal and oxygen atoms are 2.08 and 2.13 Å for $[Mg•(H_2O)_1]^+$ and $[Al•(H_2O)_1]^+$, respectively. For $[Mg•(H_2O)_2]^+$ and $[Al•(H_2O)_2]^+$, we calculate two types of isomers as shown in Figs. 2b and 2c. One is an adduct isomer (Form 2-I); the water molecules are almost intact concerning the structure, and are directly bound to the metal ion. The other is a reactive isomer (Form 2-II); the metal ion is inserted into the O–H bond of one water molecule, producing an $[HO–metal–H]^+$ ion. In the case of $[Mg•(H_2O)_2]^+$, only Form 2-I is stable; Form 2-II has a vibration with a negative frequency. On the other hand, the $[Al•(H_2O)_2]^+$ ion has both isomers of Forms 2-I and 2-II; Form 2-II is more stable than Form 2-I by 6427 cm^{-1}. Figure 3 shows comparison of the observed infrared spectra with the calculated ones for the optimized structures of $[Mg•(H_2O)_{1,2}]^+$ and $[Al•(H_2O)_{1,2}]^+$. We tabulate observed and calculated band positions in Table 1.

As shown in Fig. 3a, the $[Mg•(H_2O)_1]^+$ ion shows two bands at 3525 and 3640 cm^{-1} with the rotational contour that spreads over 3500–3700 cm^{-1}. These bands can be assigned to the symmetric and asymmetric OH stretching vibrations of the water molecule, respectively. Sodupe and Bauschlicher calculated the frequencies of these vibrations to be 3557 and 3622 cm^{-1} [2,8]. Our DFT calculation also provides the frequencies of 3533 and 3620 cm^{-1} as shown in Fig. 3b. These calculated values well reproduce the observed ones. The $[Mg•(H_2O)_1]^+$ ion has a $Mg^+•••OH_2$ structure like Form 1-I; the hydrogen atoms are free from intermolecular bonds. Compared to the case of free water, the $[Mg•(H_2O)_1]^+$ ion enhances the intensity of the symmetric vibration relative to that of the asymmetric one. The enhancement is characteristic of cation-attached water molecules [22]. The same tendency was also seen in a theoretical study; the intensity of the symmetric band relative to that of the asymmetric one was calculated to be 0.6 for the $[Mg•(H_2O)_1]^+$ ion, whereas it was 0.2 for free water [8]. However, band intensity in infrared photodissociation spectra depends also on the dissociation efficiency from vibrationally excited states. Further experimental and theoretical investigation on the photodissociation process is necessary for solving the problem of the intensity enhancement.

With respect to the $[Mg•(H_2O)_2]^+$ ion, the observed spectrum (Fig. 3c) resembles that of $[Mg•(H_2O)_1]^+$; two bands emerge at 3560 and 3645 cm^{-1}. These bands are assigned to the symmetric and asymmetric OH stretching vibrations of the water molecules. No band is observed in the region of the hydrogen-bonded OH stretching vibration (3200–3500 cm^{-1}), suggesting that there is no water–water intermolecular bond. The calculated spectrum of Form 2-I (Fig. 3d) well reproduces the observed spectrum. In the $[Mg•(H_2O)_2]^+$ ion, the water molecules are directly bound to the magnesium ion through the $Mg^+•••OH_2$ intermolecular bonds. The

$[Mg•(H_2O)_2]^+$ ion has a bent structure with the two water molecules staggered. This structure is due to polarization of the Mg^+ 3s orbital. The solvation of the first H_2O molecule to the Mg^+ ion provides the mixing of the 3s and 3p orbitals. This mixing creates an area of high electron density behind the Mg^+ ion, letting the second H_2O molecule be located on the same side of the first H_2O molecule. The similar structures were theoretically proposed in several papers [1,7,9,10].

The $[Al•(H_2O)_1]^+$ ion has a spectrum similar to that of $[Mg•(H_2O)_1]^+$; two bands are observed at 3462 and 3582 cm^{-1}. These bands are also ascribed to the symmetric and asymmetric OH stretching vibrations of the water molecule. The existence of these bands is predicted for Form 1-I (Fig. 3f). The frequencies are estimated to be 3503 and 3598 cm^{-1}. As in the $[Mg•(H_2O)_1]^+$ ion, the water molecule is bound to the aluminum ion through the intermolecular $Al^+•••OH_2$ bond. However, the vibrations of $[Al•(H_2O)_1]^+$ have frequencies slightly lower than that of $[Mg•(H_2O)_1]^+$. This shift may be due to larger water-to-metal electron donation for the Al system than for the Mg one, as mentioned by Sodupe and Bauschlicher [13]. The further the water molecule gives its electron clouds to the metal ion, the weaker the covalent bonds of the water molecule become. As a result, the intramolecular vibrations of the water molecule have lower frequencies in the $[Al•(H_2O)_1]^+$ complex.

Meanwhile, the $[Al•(H_2O)_2]^+$ ion shows spectral features different from those of the other ions investigated in this study. In the observed spectrum (Fig. 3g), there are three band maxima at 3528, 3630, and 3714 cm^{-1}. Since the positions of the lowest-frequency and the second-lowest-frequency bands are similar to the band positions of $[Mg•(H_2O)_{1,2}]^+$ and $[Al•(H_2O)_1]^+$, we assign these bands to the symmetric and asymmetric OH stretching vibrations of a water molecule that is bound directly to the aluminum ion. Apparently, the 3714-cm^{-1} band cannot be ascribed to a water

molecule that is directly bound to the aluminum ion, because the frequency is fairly higher than those of water molecules in the first solvation shell. One possible interpretation is that this band is due to a water molecule that is not directly bound to the aluminum ion; the position is similar to the asymmetric OH stretching vibration of free water (3756 cm^{-1}) [29]. However, since the observed spectrum does not show any absorption in the hydrogen-bonded OH stretching (3100–3500 cm^{-1}) region, no water–water intermolecular bond is formed in the cluster. DFT calculations predict that the most stable isomer is Form 2-II. The calculated spectrum of Form 2-II is shown in Fig. 3h. This isomer has three bands at 3519, 3613, and 3733 cm^{-1} in the 3000–3800 cm^{-1} region. The first and the second bands are assigned to the symmetric and asymmetric OH stretching vibrations of the water molecule. The third one is the OH stretching vibration of the $[HO–Al–H]^+$ ion [30]. Since the spectrum of Form 2-II well coincides with the observed one, the $[Al•(H_2O)_2]^+$ ion has a geometric structure of Form 2-II. The existence of the observed 3714-cm^{-1} band clearly shows that the insertion reaction occurs in the $[Al•(H_2O)_2]^+$ ion, producing the $[HO–Al–H]^+$ ion. In comparison of the observed spectrum (Fig. 3g) with the calculated one of Form 2-II (Fig. 3h), one can see intensity discrepancy between them. The 3714-cm^{-1} band is quite weaker than the 3528- and 3630-cm^{-1} bands, whereas the calculated intensities are comparable to each other. One explanation of the discrepancy is that it is due to the coexistence of Forms 2-I and 2-II. The existence of Form 2-I may enhance the intensities of the 3528- and 3630-cm^{-1} bands relative to that of the 3714-cm^{-1} band, because the symmetric stretching vibrations (3527 and 3527 cm^{-1}) and asymmetric ones (3627 and 3628 cm^{-1}) of Form 2-I may overlap those of Form 2-II (3519 and 3613 cm^{-1}, respectively) in the observed spectrum. In order to confirm the coexistence of these two isomers, we are planning to measure infrared spectra of larger clusters,

$[Al•(H_2O)_2•Ar_{n\geq 2}]^+$, for lowering the ion temperature. For the aluminum–water system, we can experimentally propose that the $[HO–Al–H]^+$ ion exists in $[Al•(H_2O)_{n\geq 2}]^+$. This ion-core change at $n = 2$ was predicted theoretically by Iwata et al. [16] For $n = 1$, the isomer with the Al^+ ion core is more stable than the $[HO–Al–H]^+$ ion by 49.36 kJ/mol, although the most preferable form for $n = 2$ is the isomer with the $[HO–Al–H]^+$ ion core [16].

In summary, we have investigated the structures of $[Mg•(H_2O)_{1,2}]^+$ and $[Al•(H_2O)_{1,2}]^+$ by the infrared photodissociation spectroscopy and the DFT calculations. The $[Mg•(H_2O)_{1,2}]^+$ and $[Al•(H_2O)_1]^+$ ions have the structures in which all the water molecules are directly bound to the metal ions. In the case of $[Al•(H_2O)_2]^+$, the intracluster insertion reaction occurs, producing the $[HO–Al–H]^+$ ion core.

Table 1

Observed and calculated frequencies (cm^{-1}), and calculated infrared intensities (in parentheses, km/mol).

Species	observed frequency, cm^{-1}	calculated frequency[a], cm^{-1}
$[Mg•(H_2O)_1]^+$	3525	3533 (55)
	3642	3620 (212)
$[Mg•(H_2O)_2]^+$	3560	3537 (32)[b], 3540 (20)[b]
	3645	3629 (169)[b], 3633 (179)[b]
$[Al•(H_2O)_1]^+$	3462	3503 (103)
	3582	3598 (218)
$[Al•(H_2O)_2]^+$	3528	3519 (193)[c]
	3630	3613 (319)[c]
	3714	3733 (253)[c]
	–	3527 (43)[b], 3527 (99)[b]
	–	3627 (146)[b], 3628 (212)[b]

[a] A scaling factor of 0.9654 is used.

[b] Values of Form 2-I.

[c] Values of Form 2-II.

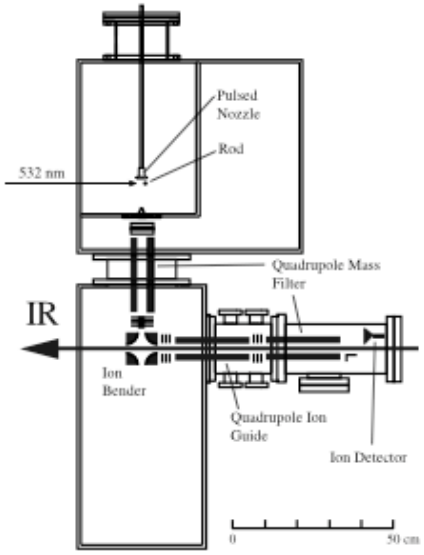

Figure 1. Inokuchi et al.

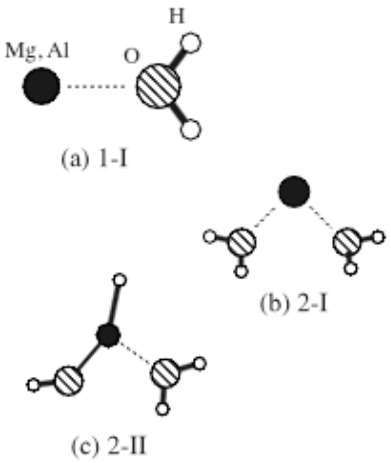

Figure 2. Inokuchi et al.

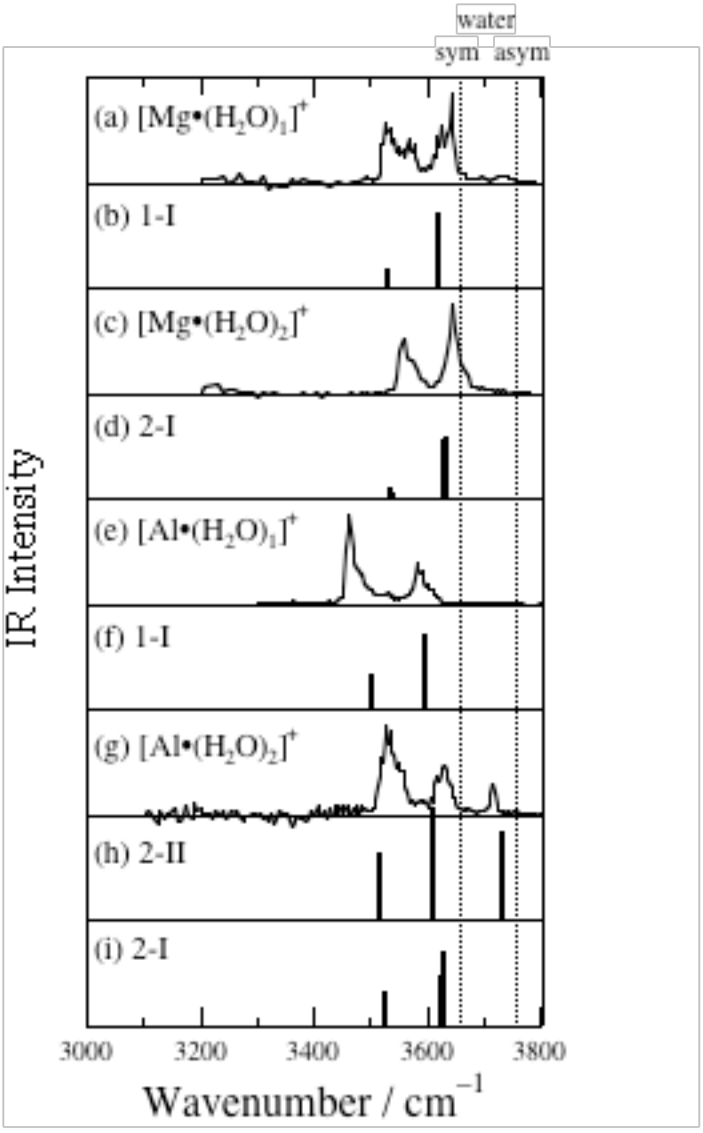

Figure 3. Inokuchi et al.

References and notes

[1] F. Misaizu, M. Sanekata, K. Tsukamoto, K. Fuke, S. Iwata, J. Phys. Chem. 96 (1992) 8259.

[2] K. F. Willey, C. S. Yeh, D. L. Robbins, J. S. Pilgrim, M. A. Duncan, J. Chem. Phys. 97 (1992) 8886.

[3] K. Fuke, F. Misaizu, M. Sanekata, K. Tsukamoto, S. Iwata, Z. Phys. D 26 (1993) S180.

[4] F. Misaizu, M. Sanekata, K. Fuke, S. Iwata, J. Chem. Phys. 100 (1994) 1161.

[5] M. Sanekata, F. Misaizu, K. Fuke, S. Iwata, K. Hashimoto, J. Am. Chem. Soc. 117 (1995) 747.

[6] C. W. Bauschlicher Jr., H. Partridge, Chem. Phys. Lett. 181 (1991) 129.

[7] C. W. Bauschlicher Jr., H. Partridge, J. Phys. Chem. 95 (1991) 9694.

[8] M. Sodupe, C. W. Bauschlicher Jr., Chem. Phys. Lett. 195 (1992) 494.

[9] C. W. Bauschlicher Jr., M. Sodupe, H. Partridge, J. Chem. Phys. 96 (1992) 4453.

[10] H. Watanabe, S. Iwata, K. Hashimoto, F. Misaizu, K. Fuke, J. Am. Chem. Soc. 117 (1995) 755.

[11] T. Asada, S. Iwata, Chem. Phys. Lett. 260 (1996) 1.

[12] F. Misaizu, K. Tsukamoto, M. Sanekata, K. Fuke, Z. Phys. D 26 (1993) S177.

[13] M. Sodupe, C. W. Bauschlicher Jr., Chem. Phys. Lett. 181 (1991) 321.

[14] H. Watanabe, M. Aoki, S. Iwata, Bull. Chem. Soc. Jpn. 66 (1993) 3245.

[15] J. Hrusák, D. Stöckigt, H. Schwarz, Chem. Phys. Lett. 221 (1994) 518.

[16] H. Watanabe, S. Iwata, J. Phys. Chem. 100 (1996) 3377.

[17] C.-K. Siu, Z.-F. Liu, J. S. Tse, J. Am. Chem. Soc. 124 (2002) 10846.

[18] L. I. Yeh, M. Okumura, J. D. Myers, J. M. Price, Y. T. Lee, J. Chem. Phys. 91 (1989) 7319.

[19] E. J. Bieske, J. P. Maier, Chem. Rev. 93 (1993) 2603.

[20] J. M. Lisy, Cluster Ions (Wiley, Chichester, 1993) p. 217.

[21] Y. Inokuchi, N. Nishi, J. Chem. Phys. 117 (2002) 10648.

[22] Y. Inokuchi, K. Ohashi, Y. Honkawa, N. Yamamoto, H. Sekiya, N. Nishi, J Phys. Chem. A 107 (2003) 4230.

[23] G. Gregoire, J. Velasquez, M. A. Duncan, Chem. Phys. Lett. 349 (2001) 451.

[24] G. Gregoire, J. Velasquez, M. A. Duncan, J. Chem. Phys. 117 (2002) 2120.

[25] G. Gregoire, N. R. Brinkmann, D. van Heijnsbergen, H. F. Schaefer, M. A. Duncan, J. Phys. Chem. A 107 (2003) 218.

[26] R. S. Walters, N. R. Brinkmann, H. F. Schaefer, M. A. Duncan, J. Phys. Chem. A 107 (2003) 7396.

[27] N. R. Walker, R. S. Walters, E. D. Pillai, M. A. Duncan, J. Chem. Phys. 119 (2003) 10471.

[28] M. J. Frisch, et al. Gaussian 98 Revision A.9, Gaussian, Inc., Pittsburgh PA, 1998.

[29] G. Herzberg, Molecular Spectra and Molecular Structure. Vol. 2. Infrared and Raman Spectra of Polyatomic Molecules (Krieger, Malabar, 1991) p. 281.

[30] The frequency of the Al–H stretching vibration of Form 2-II is calculated to be 2038 cm^{-1}.

Figure captions

Figure 1. Schematic diagram of the photodissociation spectrometer.

Figure 2. Schematic drawing of the optimized structures of $[Mg•(H_2O)_{1,2}]^+$ and $[Al•(H_2O)_{1,2}]^+$. We call these isomers (a) Form 1-I, (b) Form 2-I, and (c) Form 2-II.

Figure 3. Infrared photodissociation spectra of (a) $[Mg•(H_2O)_1•Ar]^+$, (c) $[Mg•(H_2O)_2•Ar]^+$, (e) $[Al•(H_2O)_1•Ar]^+$, and (g) $[Al•(H_2O)_2•Ar]^+$, and calculated infrared spectra of (b) Form 1-I of $[Mg•(H_2O)_1]^+$, (d) Form 2-I of $[Mg•(H_2O)_2]^+$, (f) Form 1-I of $[Al•(H_2O)_1]^+$, and (h, i) Forms 2-II and 2-I of $[Al•(H_2O)_2]^+$. The dotted lines represent band positions of the symmetric and asymmetric OH stretching vibrations of free water (3657 and 3756 cm^{-1}, respectively) [29].